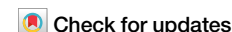


<https://doi.org/10.1038/s41612-024-00621-5>

# Position-specific isomers of monohydroxy fatty acids in the land-atmosphere interface: identification and quantification



Mutong Niu<sup>1,4</sup>, Na An<sup>2,4</sup>, Wenxin Zhang<sup>1</sup>, Wei Hu<sup>1</sup>, Xiaoli Fu<sup>1</sup>, Kimitaka Kawamura<sup>3</sup>, Yuqi Feng<sup>2</sup>, Quanfei Zhu<sup>2</sup>✉ & Pingqing Fu<sup>1</sup>✉

Due to a wide variety and similar physicochemical properties of monohydroxy saturated fatty acids (OH-FAs) isomers as biomarkers, previously reported OH-FAs in environmental samples were mainly restricted to the  $\alpha$ -,  $\beta$ -, ( $\omega$ -1)- and  $\omega$ -OH-FA isomers. Here, *N,N*-dimethylethylenediamine (DMED) labeling coupled with ultra-high-performance liquid chromatography-mass spectrometry (UHPLC-MS) analysis with multiple reaction monitoring mode (MRM) was developed to screen, identify and quantify position-specific isomers of OH-FAs (C8-C18). An identification strategy of positional isomers of OH-FAs, including  $\alpha$ -,  $\beta$ -, 4 to ( $\omega$ -2)-, ( $\omega$ -1)- and  $\omega$ -OH-FAs, was established by integrating the characteristics of peak intensity ratios of product ions based on the library of OH-FAs. Meanwhile,  $d_4$ -DMED-labeled OH-FA standards as internal standards were adopted for the relative quantification of positional isomers. The extraction processes were optimized for different interface-environmental samples. Our method offers a promising tool to investigate position-specific isomers of OH-FAs in the land-atmosphere interface.

Monohydroxy saturated fatty acids (OH-FAs) are pervasive lipid constituents found in various organisms<sup>1–3</sup> and serve as essential tracers for microorganisms and higher plants in environmental and earth science research<sup>4,5</sup>. For several decades, research has been conducted on position-specific isomers of OH-FAs, utilizing them as environmental tracers crucial for elucidating the migration processes of microorganisms and metabolites of higher plants in the surface-earth systems<sup>5–7</sup>. The compositions and concentrations of OH-FA isomers at hydroxyl positions of  $\alpha$ ,  $\beta$ , and  $\omega$  provide indications regarding the contributions from soil microorganisms<sup>8,9</sup>, gram-negative bacteria (GNB)<sup>10,11</sup> and metabolites derived from higher terrestrial plants<sup>8,12,13</sup> to environmental samples, respectively.

However, numerous OH-FA isomers exist in nature, but mid-position OH-FAs (refer to saturated fatty acids with a hydroxyl group in the middle of the carbon chain), in particular, were rarely reported<sup>4</sup>. Recent studies have highlighted their significant presence in environmental samples<sup>14–16</sup>. These mid-position OH-FAs predominantly originated from the biological processes of plants<sup>17,18</sup>, algae<sup>19,20</sup> and microbes<sup>21,22</sup>. They are integral components of cell membrane structures<sup>18,23</sup> and by-products of metabolic activities<sup>20</sup>, and may be released into the surrounding environment in response to specific physiological or environmental pressures<sup>24,25</sup>. For example, the

fungal species *Mucor rouxii* has been specifically identified to specifically generate 7-OH-C12-FA in oxygen-limited conditions<sup>26</sup>, thus suggesting that mid-position OH-FAs could potentially serve as biochemical markers for certain biological processes, possibly demonstrating microbial specificity<sup>15,27</sup>. A comprehensive analysis of OH-FA isomers in the surface-earth system is pivotal for tracing the migration processes of organisms. Moreover, since these compounds may arise from stress reactions in organisms, their detection could signify particular environmental circumstances, thereby providing valuable insights into potential environmental shifts and overall ecosystem health.

However, the comprehensive profiling of OH-FAs has been hindered by the absence of a robust analytical technique, leaving the composition of OH-FA pools in various environmental samples largely unexplored. The prevalent method for the detection of OH-FAs in the surface-earth system is to employ gas chromatography-mass spectrometry (GC-MS) after silylation, or amidation derivatization<sup>8–10</sup>. Nevertheless, this approach only allows for the detection of OH-FA isomers at the  $\alpha$ ,  $\beta$ , and  $\omega$  hydroxyl positions. Consequently, OH-FAs at other hydroxyl positions continue to elude the detection and identification, leading to a significant knowledge gap concerning mid-position OH-FA isomers, which are postulated to possess more

<sup>1</sup>Institute of Surface-Earth System Science, School of Earth System Science, Tianjin University, Tianjin 300072, China. <sup>2</sup>School of Bioengineering and Health, Wuhan Textile University, Wuhan 430072, China. <sup>3</sup>Chubu Institute for Advanced Studies, Chubu University, Kasugai, Aichi 487-8501, Japan. <sup>4</sup>These authors contributed equally: Mutong Niu, Na An. ✉e-mail: [qf\\_zhu@whu.edu.cn](mailto:qf_zhu@whu.edu.cn); [fupingqing@tju.edu.cn](mailto:fupingqing@tju.edu.cn)

distinct origins<sup>14,15,26</sup>. Liquid chromatography-mass spectrometry (LC-MS) is a powerful analytical tool for small molecular compounds due to its high sensitivity and selectivity, and broad adaptability<sup>28,29</sup>. Most recently, leveraging isotope labeling, we developed a set of screening and identification strategies for OH-FA positional isomers in biological samples based on liquid chromatography-high resolution mass spectrometry (LC-HRMS), and the library including the data of 132 position-specific isomers of OH-FAs was constructed<sup>30</sup>.

In this work, we improved and developed a more facile method for the simultaneous screening, identification, and quantification of position-specific OH-FA isomers in environmental samples (e.g., soil, leaf, pollen, and microbial samples) by combining the *N,N*-dimethylethylenediamine (DMED) labeling with ultra-high-performance LC-triple quadrupole MS (UHPLC-QqQ MS) technique. First, we established a set of multiple reaction monitoring mode (MRM) screening strategies on QqQ MS according to the fragmentation pattern of DMED-labeled OH-FAs under collision-induced dissociation (CID). Subsequently, a simple identification process for OH-FA positional isomers was established by integrating the characteristics of peak intensity ratios of product ions based on the DMED-labeled metabolite library. Finally, a relative quantitative approach was established using  $d_4$ -DMED-labeled OH-FA standards as internal standards. The established integrated techniques for screening, identification, and quantification of position-specific isomers were applied in the analysis of OH-FA pools in the land-atmosphere interface.

## Results

In this work, we started from the three aspects of screening, identification, and quantification of OH-FA positional isomers, and established a simple and rapid method to study the variations of the OH-FA pool in the land-atmosphere interface (Fig. 1). The specific method is presented as follows:

### Screening strategy for OH-FAs

Our previous studies have demonstrated that DMED labeling is an effective technique for enhancing the detection sensitivity and selectivity of carboxylated compounds in LC-MS<sup>29-31</sup>. The carboxyl group in chemical compounds can react with DMED, leading to the formation of amides. The tertiary amine, incorporated through DMED labeling, exhibits heightened protonation ability under acidic conditions, thereby improving ionization efficiency in ESI-MS within a positive ion mode. This amine also displayed special fragmentation behavior via CID, leading to the loss of either the

dimethylamine neutral fragment or the H<sub>2</sub>O neutral fragment. Owing to this distinctive fragmentation, the product ions mass spectra of DMED-labeled carboxylated compounds were clearer, and the detection sensitivities of carboxylated compounds could increase by several to hundreds of times<sup>29</sup>. Consequently, DMED was selected for the labeling of OH-FAs in environmental samples in this study.

For examining the mass spectrometry fragmentation rules of DMED-labeled OH-FAs, four OH-FA standards (3-OH-C8-FA, 8-OH-C8-FA, 3-OH-C16-FA, and 12-OH-C16-FA, the information of standards were presented in Supplementary Table 1) were selected to observe the fragmentation pattern (Fig. 2). The fragmentation of DMED-labeled OH-FAs were consistent with previous studies<sup>30</sup>, occurring primarily in the amine C-N bond and hydroxyl group, which caused the loss of the neutral fragment H<sub>2</sub>O (18 Da) and/or dimethylamine (45 Da). As a result, DMED-labeled OH-FAs generated three characteristic product ions via CID,  $[M + H]^+ - 18$ ,  $[M + H]^+ - 45$ , and  $[M + H]^+ - 63$ . For example, DMED-labeled OH-C8-FA could generate two dominant product ions at  $m/z$  186.2 ( $[M + H]^+ - 45$ ) and  $m/z$  168.2 ( $[M + H]^+ - 63$ ), and one minor product ion at  $m/z$  213.2 ( $[M + H]^+ - 18$ ) via CID (Fig. 2a, b).

Based on this special fragmentation behavior, LC-QqQ MS-based MRM mode was employed for high-sensitivity quantification of OH-FAs. In the first stage (MS1), the precursor ions (referring to DMED-labeled OH-FAs) were isolated and subsequently fragmented via CID. The information regarding DMED-labeled OH-FAs (C8-C18) can be obtained from the DEMD-labeled OH-FA library. In the second stage (MS2), three specific product ions produced from the precursor ions were separated and selected by Q3 analyzer. The  $m/z$  of product ions of DMED-labeled OH-FAs can be predicted by subtracting the neutral loss from  $m/z$  of precursor ions. Here, two product ions,  $[M + H]^+ - 45$  and  $[M + H]^+ - 63$ , were selected for subsequent analysis and the information about selected product ions was shown in Supplementary Table 2. When these two precursor-product ion pairs of an OH-FA were monitored simultaneously using MRM mode, its extracted ion chromatograms (EIC) could be obtained and OH-FAs could be picked out based on the peak pair with the same retention time (RT) and similar peak shape (Fig. 3a). Based on this, the LC-MRM-MS strategy was performed for screening OH-FAs.

### A two-step identification process

This process was proposed to achieve rapid and accurate identification of position-specific isomers: library matching and confirmation of the

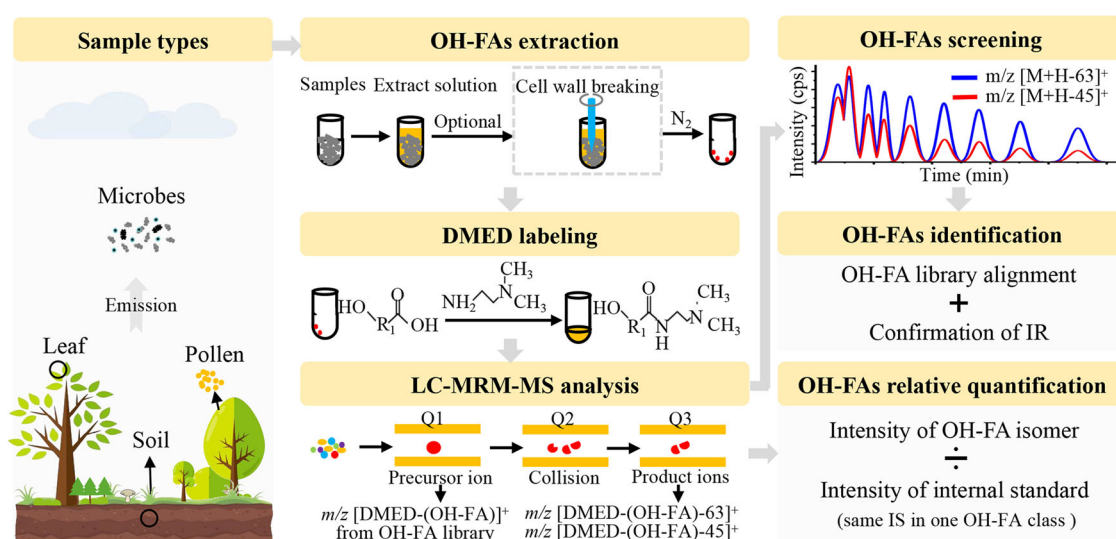


**Fig. 1 | Workflow for isomeric OH-FAs profiling in the land-atmosphere interface.** The picture presents the brief process of the developed method, including selected environmental sample types (including soil, leaf, pollen, and microbial samples), the general extraction procedure for OH-FAs, the procedure and principle

of isomeric OH-FAs detection (DMED-labeling and LC-MRM-MS analysis), as well as the overall procedure for screening, identification, and quantification of position-specific OH-FA isomers.

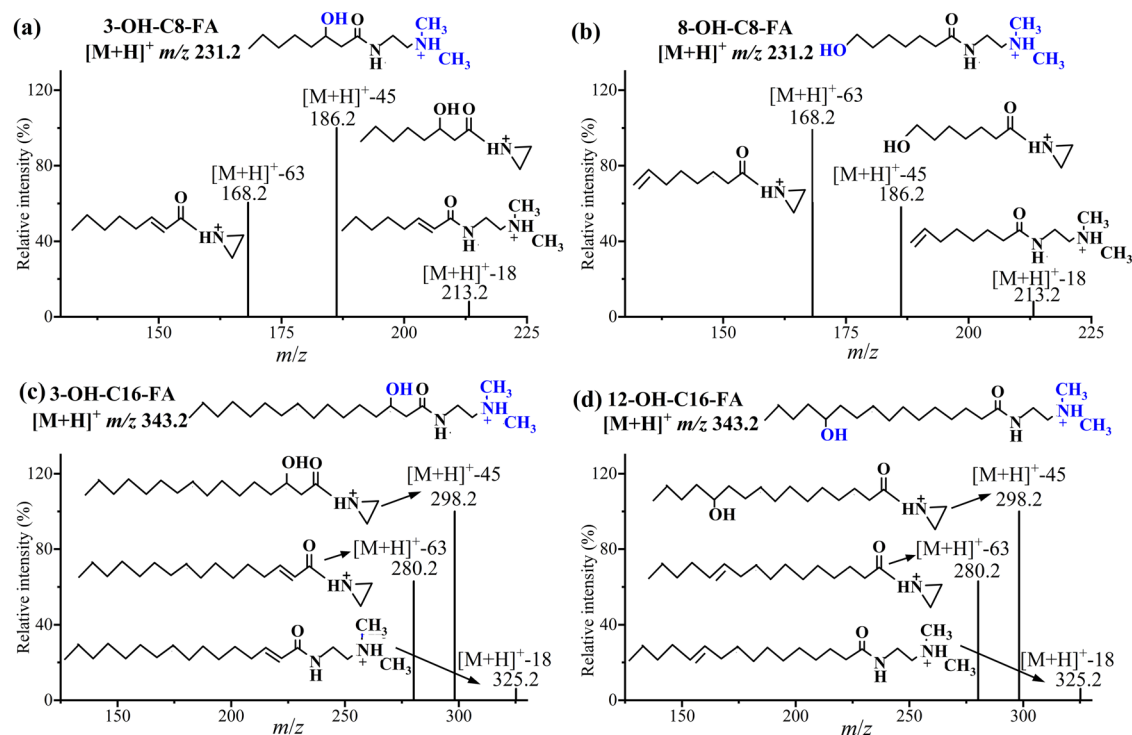


**Fig. 2 | The fragmentation pattern of DMED-labeled OH-C8-FAs and OH-C16-FAs.** MS/MS spectra of DMED-labeled **a** 3-OH-C8-FA, **b** 8-OH-C8-FA, **c** 3-OH-C16-FA, and **d** 12-OH-C16-FA at CID voltage of 30 V in AB SCIEX 6500+ triple quadrupole MS are presented, respectively. The compound abbreviation, the corresponding  $m/z$  and the chemical structure after DMED labeling are presented above

each panel. The blue parts of the chemical structure are the parts lost under collision-induced dissociation (CID). The  $m/z$  of the three fragment ions of the DMED-labeled OH-FAs and the structures of the fragmented compounds are presented in panels.

intensity ratio of product ions. A library including information on the structure and  $m/z$  of position-specific isomers of OH-FAs, as well as retention index (RI) and major product ions of DMED-labeled OH-FAs has previously been established to facilitate the identification. Of the information recorded in the library, the RI values could calibrate to some extent the drift of retention time in the LC-MS analysis of different batches, which provides comparable chromatographic retention values for the identification of OH-FA positional isomers. Thus, by comparing the RI values of OH-FA candidates from a given OH-FA class with the RI values provided by the OH-FA library within the relative error tolerance (RE) range of < 1.5%, we could achieve a preliminary identification of OH-FA positional isomers. As an example, 12 peak pairs were screened in the extracted ion chromatograms (EIC) of OH-C13-FAs in samples (Fig. 3a). The RI values of 12 OH-FA isomers were calculated and compared with the library. Within RE < 1.5%, 9 peak pairs (peak 4–12) were assigned to 12-OH-C13-FA (RE, 1.1%), 10/13-OH-C13-FA (RE, 0.1/0.5%), 9-OH-C13-FA (RE, 0.3%), 8-OH-C13-FA (RE, 0.7%), 6-OH-C13-FA (RE, 0.7%), 5-OH-C13-FA (RE, 1.2%), 4-OH-C13-FA (RE, 0.9%), and 3-OH-C13-FA (RE, 0.3%), respectively (Fig. 3b).

For further auxiliary identification of the OH-FA positional isomers, the intensity ratio of the product ions ( $I_{[M+H]^+ \rightarrow [M+H-63]^+} / I_{[M+H]^+ \rightarrow [M+H-45]^+}$ , IR) is introduced into the identification process. IR is known to show an inverse U-shape variation with the hydroxyl position of OH-FAs<sup>30</sup>. When the hydroxyl position is closer to ( $\alpha$ -/ $\beta$ -) or farther away from ( $(\omega-1)$ -/ $\omega$ -) the carboxylic acid group in the structure of OH-FAs, the neutral fragments  $H_2O$  is more difficult to lose and the intensity of product ion ( $[M+H]^+ - 45$ ) is relatively higher. Since the IR produced by different mass spectrometers is not identical, we reconstructed an auxiliary identification system of IR versus hydroxyl positions applicable to this study by counting the IR values of 38 OH-FA standards, and initially categorized five intervals of IR values for  $\alpha$ -,  $\beta$ -, 4 to ( $\omega-2$ )-, ( $\omega-1$ )-, and  $\omega$ -OH-FAs (Fig. 3c). This evaluation criterion of the identification of IR values was used for further confirmation.

As an example, the IR values of the peak pairs (peak 4, 6–12, Fig. 3b) all fell within the intervals of IR values we established using the standards. And the IR value of peak 5 was 3.3, which fell in the IR interval of 4 to ( $\omega-2$ )-OH-FAs. Thus, the peak 5 was assigned to 10-OH-C13-FA. In summary, a set of protocols for the identification of position-specific OH-FA isomers was carried out (Fig. 3d). Compared with previous methods, this developed method could detect all OH-FA isomers simultaneously and had relatively higher sensitivity (Supplementary Table 3).

### Relative quantification

In this study, OH-FAs labeled with  $d_4$ -DMED as internal standards were added before LC-MS injection to calibrate the shift of mass spectral signals during LC-MS analysis (Supplementary Table 1). As shown in Supplementary Table 4, the correlation coefficients ( $R^2$ ) for 38 OH-FA standards were between 0.9851 and 0.9998, illustrating excellent linearities. Given the constraint of having only 38 internal standards, for each OH-FA class, we strategically selected one internal standard as the reference to calibrate the mass spectral signal of other isomers within that class for which no individual internal standard was available. The proposed method allows to obtain relative quantitative information for all detectable OH-FA positional isomers in a single analysis.

### Evaluation of extraction solvents

To design rational extraction processes, four pure solvents and three extractive mixtures matching the polarity index and solubility of OH-FAs were selected to obtain the best performance of OH-FAs extraction from different interface-environmental samples (Fig. 4a). The results showed that 41 OH-FAs with ethyl acetate (EtOAc), 18 with methanol (MeOH), 37 with dichloromethane (DCM), 9 with acetonitrile (ACN), 36 with DCM/MeOH (v/v, 2:1) and 54 with DCM/MeOH (v/v, 9:1) were detected in the extracts from soil samples. Since more OH-FA positional isomers can be extracted with DCM/MeOH (v/v, 9:1), this solvent was subsequently used to extract

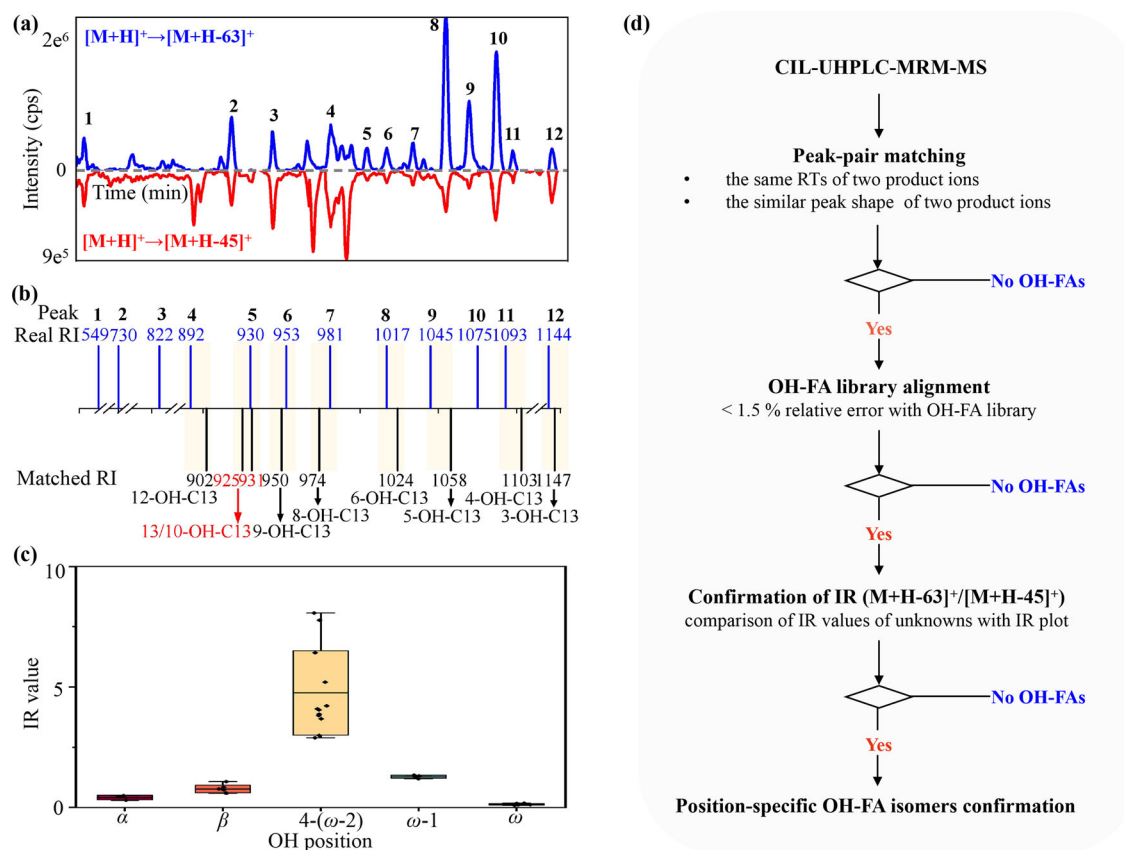


**Fig. 3 | The identification process for OH-C13-FA positional isomers. a** Extracted ion chromatogram of OH-C13-FA. **b** The comparison of calculated RI values of OH-C13-FA candidates with the RI values provided by the OH-FA library within

RE < 1.5%. **c** Distribution of IR values versus hydroxyl positions of 38 OH-FA standards. **d** The proposed identification strategy for position-specific OH-FA isomers.

the OH-FAs from soil samples. There were 41 and 54 OH-FAs with EtOAc, 28 and 49 with MeOH, 33 and 52 with DCM, and 26 and 44 with ACN detected from leaf and pollen, respectively, resulting in EtOAc as an extraction solution for plant samples.

For microbial samples, the pre-treatment methods for bacteria and fungi were optimized separately because of differences in cell structure. We detected 54 and 31 OH-FAs with EtOAc, 39 and 27 with MeOH, 43 and 31 with DCM, 51 and 45 with ACN, 60 and 54 with DCM/MeOH (v/v, 9:1), 47 and 34 with DCM/MeOH (v/v, 2:1), and 63 and 49 with methyl tert-butyl ether (MTBE)/MeOH/H<sub>2</sub>O (v/v/v, 10:3:2.5) from bacteria and fungi samples, respectively. Therefore, MTBE/MeOH/H<sub>2</sub>O was selected to extract OH-FAs from microbial samples. Polar solvents penetrate cells more easily than non-polar solvents, allowing better contact between lipids and the solvent<sup>32</sup>, but the increase in solvent polarity may not be effective in extracting more lipids<sup>33</sup>, and medium-polarity solvents (EtOAc and DCM) extracted more OH-FA positional isomers (Supplementary Fig. 1). Therefore, mixed solvents are more suitable for the extraction of OH-FAs from complex environmental samples.

### Evaluation of disruption method

To obtain more position-specific OH-FA isomers from biological cells, a suitable cell disruption method is needed to enhance the release of intracellular OH-FAs from microbial samples<sup>34</sup>. Mechanical methods such as microwave, ultrasonication, autoclaving, and bead-beating, and non-mechanical ones such as chemical treatments and enzymatic lysis have been widely used for cell wall breaking<sup>35</sup>. For avoiding the introduction of impurities during non-mechanical processes, the four mechanical disruption methods for OH-FAs extraction from different biological samples were evaluated as described in Supplementary Methods. The results showed that sonication<sup>b</sup> (sonication using ultrasonic homogenizer; more detailed

information in Supplementary Methods) and temperature difference methods can effectively separate airbags from pollen and break the main body of pollen grains (Supplementary Figure 2), and thus more OH-FA positional isomers were obtained by sonication<sup>b</sup> disruption method. For microorganisms, it can be seen from Fig. 4a that both sonication<sup>b</sup> (bacteria: 62, fungi: 52) and autoclaving (bacteria: 63, fungi: 54) methods can detect more OH-FA isomers. Compared with autoclaving, the product ions in the mass spectra were cleaner after sonication<sup>b</sup> treatment (Supplementary Figure 3). Thus, sonication<sup>b</sup> treatment was selected to disrupt biological samples. To increase the number of OH-FA positional isomers detected, this study proposes the extraction protocols of targeted OH-FAs in different interface-environmental samples for LC-MS analysis by combining optimal extraction solvents and disruption methods (Fig. 4b). The extraction recoveries in different interface-environmental samples (i.e., soil, plant, and microbe) were 76–135%, 71–125%, and 74–129%, which verified that the proposed methods were effective for extracting OH-FAs (Supplementary Table 5).

### Method application

With the aid of the established UHPLC-MRM-MS method and a two-step identification process, a total of 58, 39, 57, 63, and 58 species of OH-FA positional isomers were detected in soil, leaf, pollen, bacteria, and fungi samples (Fig. 5a and Supplementary Table 6), respectively. Taken together, among all detected OH-FA positional isomers, 29 isomers have been extensively studied and 65 isomers were barely reported in the past (Fig. 5b). The previously neglected isomers, mainly mid-hydroxyl position OH-FAs, were speculated to be ubiquitous<sup>15</sup>. For example, 4-OH-FAs and 5-OH-FAs mainly appear in the  $\beta$ -oxidation cycle of yeast and fungi<sup>36</sup>, while 7-OH-C12-FA is a special compound in *Mucor rouxii* related to anaerobic conditions<sup>36</sup>. In particular, the differences in the isomeric composition of





different environmental samples were mainly found in mid-hydroxyl position OH-FAs (Fig. 5c). Principal component analysis (PCA) revealed a greater similarity in the OH-FA pools collected from leaf, pollen, and microbial samples, while the soil samples exhibit noticeable differences in this regard. The isomers with substantial loadings on the principal components (PC) were mainly OH-C14-FAs and OH-C16-FAs, suggesting that their contents may vary significantly between different types of environmental samples (Fig. 5d). According to the uniqueness of the isomers (Fig. 5b), it can be found that the special isomers in soil samples are mainly OH-FAs with the hydroxyl group at the terminal position (such as 6-OH-C9-FA, 8-OH-C10-FA, 12-OH-C13-FA, 14-OH-C15-FA, and 15-OH-C18-FA), whereas samples collected from organisms (including leaf, pollen, bacteria, and fungi) were primarily characterized by 2-OH-C15/17-FAs and mid-position OH-C15/17-FAs (such as 9–11-C15-FAs and 9-C17-FAs), implying their potential specificity.

Meanwhile, Fig. 5a showed that among the even carbon-numbered OH-FAs, OH-C16-FAs and OH-C18-FAs family were the most common OH-FAs. Among all odd carbon-numbered OH-FAs, OH-C9-FAs family showed the richest isomeric diversity, while position-specific OH-C13-FA and OH-C17-FA isomers seemed to appear less in biological samples. Previous studies found that even-to-odd carbon preference in concentrations of  $\beta$ - and  $\omega$ -OH-FAs represented potential microbial origin<sup>9,37</sup>. A strong even carbon-numbered predominance (C16 > C18 > C14) with a proportion of 56–63% was also found in the formula numbers of positional isomers in this study, possibly also demonstrating a strong microbial origin<sup>12,37,38</sup>. However, due to a lack of information on the compositions of position-specific OH-FA isomers in organisms, it is still unavailable to conclude whether these isomers are derived from specific organisms or not.

## Discussion

Due to numerous position-specific isomers and their similar properties, previously reported OH-FAs in environmental samples were mainly restricted to the  $\alpha$ -,  $\beta$ -, ( $\omega$ -1)- and  $\omega$ -OH-FA isomers. We developed a comprehensive profiling of OH-FAs using UHPLC-QqQ-MS in MRM mode. Our current method specifically identified potential OH-FAs by aligning peaks of two characteristic product ions. For identifying the hydroxyl position of OH-FAs, an identification strategy was proposed based on the OH-FA library and specific MS fragmentation behavior of DMED-labeled OH-FAs. This method has been well adapted for use in different environmental samples. Under this method, a total of 94 positional-specific isomers of OH-FAs were successfully detected and annotated from interface-environmental samples, among which 38 isomers were further confirmed by standards.

This study reports the screening, identification, and quantification of multiple positional isomers including  $\alpha$ -,  $\beta$ -, 4 to ( $\omega$ -2)-, ( $\omega$ -1)-, and  $\omega$ -OH-FAs in the land-atmosphere interface. Such position-specific isomers are closely related to endemic biological materials. Such information is the key to understanding the role of the emission sources of biological particles in the ambient air, and the detailed molecular composition of natural organic matter in soil and air bodies. For example, primary biological aerosols including airborne pollen, fungal spores, and bacteria are important components of organic aerosols in the Earth's atmosphere, both in the urban boundary layer and pristine regions<sup>39,40</sup>. Thus, our study provides a methodology for obtaining a detailed spectrum of lipid biomarkers, which favors the investigation of migration processes of organisms and their metabolites in complex environment matrices in the future.

## Methods

### Chemicals and reagents

The OH-FA standards and saturated fatty acid (SFA) standards were purchased from Sigma-Aldrich Corp. (St. Louis, MO, USA), J&K Chemical Co., Ltd. (Beijing, China), and Kamel Pharmaceutical Co., Ltd. (Chengdu, China). The  $d_4$ -DMED-labeled OH-FA standards and the  $d_4$ -DMED-labeled SFA standards were prepared according to the previous reports<sup>41,42</sup>. The information on OH-FA standards and SFA standards is presented in

Supplementary Table 1 and Supplementary Table 7, respectively. Analytical grade 2-chloro-1-methylpyridinium iodide (CMPI), triethylamine (TEA), DMED, formic acid (FA), HPLC-grade ACN, EtOAc, DCM and MTBE, and LC/MS-grade MeOH were purchased from Aladdin Chemistry Co., Ltd. (Shanghai, China).

### Samples preparation

Soil, leaf, pollen, and microbe samples were selected as characteristic samples in the land-atmosphere interface environment in this study. Soil and leaf samples (*Euonymus japonicus* Thunb.) were collected from Tianjin University campus (39.11°N, 117.16°E). Pine pollen (*Pinus tabuliformis* Carr.) was collected in Mt. Changbai (42.40°N, 128.47°E; about 736 m above the ground level). Pure microbe samples (including bacteria *Pantoea vagans* and fungi *Aspergillus niger*) were obtained by purifying the microorganisms collected over Tianjin University (39.11°N, 117.16°E). More details on the sample collection and the OH-FAs extraction are provided in Supplementary Methods. The extracts of OH-FAs from the samples were dried under a nitrogen stream.

### DMED labeling

The dried residues were dissolved in 100  $\mu$ L ACN, and then 10  $\mu$ L CMPI (20 mmol L<sup>-1</sup>) and 20  $\mu$ L TEA (20 mmol L<sup>-1</sup>) were added. After vortexing for 3 min, 20  $\mu$ L DMED (20 mmol L<sup>-1</sup>) was added to derivatize OH-FAs for 1 h at 40°C, and then the solution was dried under a nitrogen stream. The dried DMED-labeled sample was redissolved in 100  $\mu$ L ACN/water (v/v, 1/9), which contain 2  $\mu$ L of 50  $\mu$ M  $d_4$ -DMED-labeled OH-FA internal standards and 1  $\mu$ L of 50  $\mu$ M  $d_4$ -DMED-labeled SFA standards. Finally, 10  $\mu$ L of the sample was loaded for UHPLC-MS analysis.

### UHPLC-MS analysis

The UHPLC-MS system consists of an ACQUITY UPLC I-Class LC (Waters, Milford, MA, USA) and an AB SCIEX 6500+ triple quadrupole MS (AB SCIEX, Framingham, MA, USA). ACQUITY HPLC HSS T3 column (1.8  $\mu$ m, 2.1 mm $\times$ 50 mm, Thermo Fisher Scientific, CA, USA) was selected to separate the target compounds. The mobile phase of (A) FA/water (v/v, 0.1/100) and (B) ACN were applied to elute the target compounds and the gradient was as follows: 0–3 min at 5% B, 3–15 min from 22% to 60% B, 15–17 min at 60% B, 17–24 min at 95% B, 24–40 min at 5% B. The flow rate was set at 0.4 mL min<sup>-1</sup>. The mass spectrometer was equipped with an electron spray ionization (ESI) source and performed in positive ion mode with MRM. The parameters for ESI source were as follows: curtain gas, 35 L min<sup>-1</sup>; collision gas, 8 L min<sup>-1</sup>; ion spray voltage, 5500 V; temperature, 500 °C; ion source gas 1, 50 L min<sup>-1</sup>; ion source gas 2, 45 L min<sup>-1</sup>. The MRM parameters for every target compound are provided in Supplementary Table 2. Data acquisition and quantification were performed using SCIEX OS v2.0.1 software. The RI values of OH-FA candidates were calculated using Eq. (1):

$$RI(\%) = [n + (t_{OH-FA} - t_{SFA(n)}) / (t_{SFA(n+1)} - t_{SFA(n)})] * 100 \quad (1)$$

where  $t_{OH-FA}$  is the RT of the target compound,  $n$  and  $t_{SFA(n)}$  is the carbon number and RT of the SFA whose RT is less than the RT of the target compound, respectively, and  $t_{SFA(n+1)}$  is the RT of the SFA whose RT is greater than the RT of the target compound.

### Method performance assessment

The mixture solution of 38 OH-FA standards was used to evaluate the accuracy of the relative quantification. DMED-labeled OH-FA standards and  $d_4$ -DMED-labeled internal standards were mixed at different molar ratios (1:50, 1:25, 1:10, 1:5, 2:1, 1:1, 5:1, 10:1, and 50:1). The regression curves were constructed by plotting peak area of light/heavy versus the mean molar ratios of light/heavy and calculated using 1/x weight analysis. The good linear relationship ( $R^2 > 0.98$ ) was shown in Supplementary Table 3. The recoveries (RR) were calculated with standards spiked in different extraction solvents at three different molar ratios (1:10, 1:1, and 10:1) according to the

following Eq. (2):

$$RR(\%) = [(M_S - M_{BS})/M_{STD}] * 100 \quad (2)$$

where  $M_S$  and  $M_{BS}$  represent the molar ratios of the different analytes in the spiked and non-spiked solvents, respectively, and  $M_{STD}$  represents the molar ratio of the different standards. All data about the method assessment is shown in Supplementary Tables 4–5.

### Statistical analysis

PCA analysis was employed using the Bray-Curtis method to visually assess the similarity of compounds among different environmental sample types. PC1 and PC2 were extracted, capturing the most substantial variance within the dataset. PCA plot was then generated, plotting PC1 against PC2, allowing for the visualization of relationships and potential clusters among the samples based on their compound profiles. The Veen and PCA plotting were performed using Origin v8.0.

### Data availability

All data that support the findings of this study are available within the manuscript and supplementary information.

Received: 9 August 2023; Accepted: 8 March 2024;

Published online: 21 March 2024

### References

- Guo, L., Zhang, X., Zhou, D. Q., Okunade, A. L. & Su, X. Stereospecificity of fatty acid 2-hydroxylase and differential functions of 2-hydroxy fatty acid enantiomers. *J. Lipid Res.* **53**, 1327–1335 (2012).
- Kim, K. R. & Oh, D. K. Production of hydroxy fatty acids by microbial fatty acid-hydroxylation enzymes. *Biotechnol. Adv.* **31**, 1473–1485 (2013).
- Oh, H. J. et al. Biotransformation of linoleic acid into hydroxy fatty acids and carboxylic acids using a linoleate double bond hydratase as key enzyme. *Adv. Synth. Catal.* **357**, 408–416 (2015).
- Kawamura, K. & Gagosian, R. B. Identification of isomeric hydroxy fatty acids in aerosol samples by capillary gas chromatography—mass spectrometry. *J. Chromatogr. A* **438**, 309–317 (1988).
- Kawamura, K. & Ishiwatari, R. Tightly bound  $\beta$ -hydroxy acids in a recent sediment. *Nature* **297**, 144–145 (1982).
- Kawamura, K., Ishiwatari, R. & Ogura, K. Early diagenesis of organic matter in the water column and sediments: Microbial degradation and resynthesis of lipids in Lake Haruna. *Org. Geochem.* **11**, 251–264 (1987).
- Eglinton, G., Hunneman, D. H. & Douraghi Zadeh, K. Gas chromatographic-mass spectrometric studies of long chain hydroxy acids-II: The hydroxy acids and fatty acids of a 5000-year-old lacustrine sediment. *Tetrahedron* **24**, 5929–5941 (1968).
- Tyagi, P., Kawamura, K., Bikkina, S., Mochizuki, T. & Aoki, K. Hydroxy fatty acids in snow pit samples from Mount Tateyama in central Japan: Implications for atmospheric transport of microorganisms and plant waxes associated with Asian dust. *J. Geophys. Res.* **121**, 13641–13660 (2016).
- Tyagi, P., Yamamoto, S. & Kawamura, K. Hydroxy fatty acids in fresh snow samples from northern Japan: Long-range atmospheric transport of Gram-negative bacteria by Asian winter monsoon. *Biogeosci. Disc.* **12**, 13375–13397 (2015).
- Uhlig, S. et al. Profiling of 3-hydroxy fatty acids as environmental markers of endotoxin using liquid chromatography coupled to tandem mass spectrometry. *J. Chromatogr. A* **1434**, 119–126 (2016).
- Kutschera, A. et al. Bacterial medium-chain 3-hydroxy fatty acid metabolites trigger immunity in *Arabidopsis* plants. *Science* **364**, 178–181 (2019).
- Tyagi, P., Ishimura, Y. & Kawamura, K. Hydroxy fatty acids in marine aerosols as microbial tracers: 4-year study on  $\beta$ - and  $\omega$ -hydroxy fatty acids from remote Chichijima Island in the western North Pacific. *Atmos. Environ.* **115**, 89–100 (2015).
- Tyagi, P. et al. Impact of biomass burning on soil microorganisms and plant metabolites: a view from molecular distributions of atmospheric hydroxy fatty acids over Mount Tai. *J. Geophys. Res.* **121**, 2684–2699 (2016).
- Zelles, L. Identification of single cultured microorganisms based on their whole community fatty acid profiles, using an extended extraction procedure. *Chemosphere* **39**, 665–682 (1999).
- Zelles, L., Bai, Q. Y., Beck, T. & Beese, F. Signature fatty acids in phospholipids and lipopolysaccharides as indicators of microbial biomass and community structure in agricultural soils. *Soil Biol. Biochem.* **24**, 311–323 (1992).
- Zelles, L. et al. Microbial biomass, metabolic activity and nutritional status determined from fatty acid patterns and poly-hydroxybutyrate in agriculturally-managed soils. *Soil Biol. Biochem.* **26**, 439–446 (1994).
- Dembitsky, V. M., Řezanka, T. & Shubin, E. E. Unusual Hydroxy fatty acids from some higher fungi. *Phytochemistry* **34**, 1057–1059 (1993).
- Franke, R. et al. Apoplastic polyesters in *Arabidopsis* surface tissues—A typical suberin and a particular cutin. *Phytochemistry* **66**, 2643–2658 (2005).
- Gelin, F., Volkman, J. K., De Leeuw, J. W. & Sinninghe Damsté, J. S. Mid-chain hydroxy long-chain fatty acids in microalgae from the genus *Nannochloropsis*. *Phytochemistry* **45**, 641–646 (1997).
- Speelman, E. N., Reichart, G. J., de Leeuw, J. W., Rijpstra, W. C. & Sinninghe Damsté, J. S. Biomarker lipids of the freshwater fern *Azolla* and its fossil counterpart from the Eocene Arctic Ocean. *Org. Geochem.* **40**, 628–637 (2009).
- Zelles, L. Identification of single cultured micro-organisms based on their whole-community fatty acid profiles, using an extended extraction procedure. *Chemosphere* **39**, 665–682 (1999).
- Bowman, J. P., Skerratt, J. H., Nichols, P. D. & Sly, L. I. Phospholipid fatty acid and lipopolysaccharide fatty acid signature lipids in methane-utilizing bacteria. *FEMS Microbiol. Lett.* **85**, 15–21 (1991).
- Gunstone, F. D., Harwood, J. L. & Padley, F. B. *The Lipid Handbook* (Chapman and Hall, 1994).
- Guezennec, J. & Fiala-Medioni, A. Bacterial abundance and diversity in the Barbados Trench determined by phospholipid analysis. *FEMS Microbiol. Ecol.* **19**, 83–93 (1996).
- Huang, H. et al. Chemical composition of the cuticular membrane in guava fruit (*Psidium guajava* L.) affects barrier property to transpiration. *Plant Physiol. Biochem.* **155**, 589–595 (2020).
- Jeennor, S., Laoteng, K., Tanticharoen, M. & Cheevadhanarak, S. Comparative fatty acid profiling of *Mucor rouxii* under different stress conditions. *FEMS Microbiol. Lett.* **259**, 60–66 (2006).
- Zhang, W. X. et al. Hydroxy fatty acids in the surface Earth system. *Sci. Total Environ.* **906**, 167358 (2024).
- Zhang, T. Y. et al. Derivatization for liquid chromatography-electrospray ionization-mass spectrometry analysis of small-molecular weight compounds. *Trends Anal. Chem.* **119**, 115608 (2019).
- Zhu, Q. F. et al. Analysis of liposoluble carboxylic acids metabolome in human serum by stable isotope labeling coupled with liquid chromatography-mass spectrometry. *J. Chromatogr. A* **1460**, 100–109 (2016).
- Zhu, Q. F., An, N. & Feng, Y. Q. In-depth annotation strategy of saturated hydroxy fatty acids based on their chromatographic retention behaviors and MS fragmentation patterns. *Anal. Chem.* **92**, 14528–14535 (2020).
- Zhu, Q. F. et al. Analysis of cytochrome P450 metabolites of arachidonic acid by stable isotope probe labeling coupled with ultra

- high-performance liquid chromatography/mass spectrometry. *J. Chromatogr. A* **1410**, 154–163 (2015).
32. Tang, Y. et al. Efficient lipid extraction and quantification of fatty acids from algal biomass using accelerated solvent extraction (ASE). *RSC Adv.* **6**, 29127–29134 (2016).
  33. Hidalgo, P., Ciudad, G. & Navia, R. Evaluation of different solvent mixtures in esterifiable lipids extraction from microalgae *Botryococcus braunii* for biodiesel production. *Bioresour. Technol.* **201**, 360–364 (2016).
  34. Hwangbo, M. & Chu, K. H. Recent advances in production and extraction of bacterial lipids for biofuel production. *Sci. Total Environ.* **734**, 139420 (2020).
  35. Patel, A., Mikes, F. & Matsakas, L. An overview of current pretreatment methods used to improve lipid extraction from oleaginous microorganisms. *Molecules* **23**, 1562 (2018).
  36. An, J. U. & Oh, D. K. Increased production of  $\gamma$ -lactones from hydroxy fatty acids by whole *Waltomyces lipofer* cells induced with oleic acid. *Appl. Microbiol. Biotechnol.* **97**, 8265–8272 (2013).
  37. Kawamura, K., Ishimura, Y. & Yamazaki, K. Four years' observations of terrestrial lipid class compounds in marine aerosols from the western North Pacific. *Glob. Biogeochem. Cycles* **17**, 1–19 (2003).
  38. Bikkina, P., Kawamura, K., Bikkina, S. & Tanaka, N. Hydroxy fatty acids in rainwater and aerosols from suburban Tokyo in central Japan: The impact of long-range transport of soil microbes and plant waxes. *ACS Earth Space Chem.* **5**, 257–267 (2021).
  39. Schneider, J. et al. Mass-spectrometric identification of primary biological particle markers and application to pristine submicron aerosol measurements in Amazonia. *Atmos. Chem. Phys.* **11**, 11415–11429 (2011).
  40. Pöhlker, C., Huffman, J. A., Forster, J. D. & Pöschl, U. Autofluorescence of atmospheric bioaerosols: spectral fingerprints and taxonomic trends of pollen. *Atmos. Meas. Tech.* **6**, 3369–3392 (2013).
  41. Hao, Y. H. et al. Stable isotope labeling assisted liquid chromatography–electrospray tandem mass spectrometry for quantitative analysis of endogenous gibberellins. *Talanta* **144**, 341–348 (2015).
  42. Zhu, Q. F. et al. Method to calculate the retention index in hydrophilic interaction liquid chromatography using normal fatty acid derivatives as calibrants. *Anal. Chem.* **91**, 6057–6063 (2019).

## Acknowledgements

We acknowledge support from the National Natural Science Foundation of China (Grant nos. 42221001 and 41977183).

## Author contributions

M.N. and W.Z. executed sampling. M.N., N.A., W.Z., and X.F. performed the analysis. M.N., N.A., W.H., and Q.Z. drafted the paper. Q.Z., Y.F., and P.F. conceptualized the study. All authors contributed to the discussions and manuscript writing.

## Competing interests

The authors declare no competing interests.

## Additional information

**Supplementary information** The online version contains supplementary material available at <https://doi.org/10.1038/s41612-024-00621-5>.

**Correspondence** and requests for materials should be addressed to Quanfei Zhu or Pingqing Fu.

**Reprints and permissions information** is available at <http://www.nature.com/reprints>

**Publisher's note** Springer Nature remains neutral with regard to jurisdictional claims in published maps and institutional affiliations.

**Open Access** This article is licensed under a Creative Commons Attribution 4.0 International License, which permits use, sharing, adaptation, distribution and reproduction in any medium or format, as long as you give appropriate credit to the original author(s) and the source, provide a link to the Creative Commons licence, and indicate if changes were made. The images or other third party material in this article are included in the article's Creative Commons licence, unless indicated otherwise in a credit line to the material. If material is not included in the article's Creative Commons licence and your intended use is not permitted by statutory regulation or exceeds the permitted use, you will need to obtain permission directly from the copyright holder. To view a copy of this licence, visit <http://creativecommons.org/licenses/by/4.0/>.

© The Author(s) 2024